

# Depolarization and polarization transfer rates for the $C_2$ ( $X^1\Sigma_g^+$ , $a^3\Pi_u$ ) + $H(^2S_{1/2})$ collisions in the solar photosphere

S. Qutub<sup>1</sup>, Y.N. Kalugina<sup>2,3</sup>, M. Derouich<sup>1</sup>

<sup>1</sup> Astronomy and Space Science Department, Faculty of Science, King Abdulaziz University, P.O. Box 80203, Jeddah 21589, Saudi Arabia

<sup>2</sup> Department of Optics and Spectroscopy, Tomsk State University, 36 Lenin av., Tomsk 634050, Russia

<sup>3</sup> Institute of Spectroscopy, Russian Academy of Sciences, Fizicheskaya St. 5, 108840 Troitsk, Moscow, Russia

XXXX / XXXX

## ABSTRACT

**Context.** This paper is a continuation of a series of studies investigating collisional depolarization of solar molecular lines like those of MgH, CN and  $C_2$ . It is focused on the case of the solar molecule  $C_2$  which exhibits striking scattering polarization profiles although its intensity profiles are inconspicuous and barely visible. In fact, interpretation of the  $C_2$  polarization in terms of magnetic fields is incomplete due to the almost complete lack of collisional data.

**Aims.** This work aims at accurately computing the collisional depolarization and polarization transfer rates for the  $C_2$  ( $X^1\Sigma_g^+$ ,  $a^3\Pi_u$ ) by isotropic collisions with hydrogen atoms  $H(^2S_{1/2})$ . We also investigate the solar implications of our findings.

**Methods.** We utilize the MOLPRO package to obtain potential energy surfaces (PESs) for the electronic states  $X^1\Sigma_g^+$  and  $a^3\Pi_u$  of  $C_2$ , and the MOLSCAT code to study the quantum dynamics of the  $C_2$  ( $X^1\Sigma_g^+$ ,  $a^3\Pi_u$ ) +  $H(^2S_{1/2})$  systems. We use the tensorial irreducible basis to express the resulting collisional cross-sections and rates. Furthermore, sophisticated genetic programming techniques are employed to determine analytical expressions for the temperature and total molecular angular momentum dependence of these collisional rates.

**Results.** We obtain quantum depolarization and polarization transfer rates for the  $C_2$  ( $X^1\Sigma_g^+$ ,  $a^3\Pi_u$ ) +  $H(^2S_{1/2})$  collisions in the temperature range  $T = 2,000 - 15,000$  K. We also determine analytical expressions giving these rates as functions of the temperature and total molecular angular momentum. In addition, we show that isotropic collisions with neutral hydrogen can only partially depolarize the lower state of  $C_2$  lines, rather than completely. This highlights the limitations of the approximation of neglecting lower-level polarization while modeling the polarization of  $C_2$  lines.

**Conclusions.** Isotropic collisions with neutral hydrogen atoms are fundamental ingredient for understanding  $C_2$  polarization.

**Key words.** Collisions – Magnetic fields – Atomic processes – Polarization – Sun: photosphere – Line: formation

## 1. Introduction

Highly sensitive spectro-polarimetric telescopes have opened new observation windows on the lines of MgH, CN, and  $C_2$  molecules with unprecedented spatial and spectral resolutions (e.g. Stenflo, 1994; Gandorfer 2000; Berdyugina, Stenflo, & Gandorfer 2002; Faurobert & Arnaud 2003; Berdyugina & Fluri 2004; Asensio Ramos & Trujillo Bueno 2005; Trujillo Bueno et al. 2006; Milić & Faurobert 2012; Wiegmann et al. 2014; Wöger et al. 2021). Furthermore, Hanle effect on molecular polarized solar lines provides a good opportunity to determine spatially unresolved magnetic fields given the diverse magnetic sensitivities of molecular lines observed within narrow spectral regions. In fact, observation and interpretation of molecular  $C_2$  lines of the Swan system ( $d^3\Pi_u - a^3\Pi_u$ ) around 5141 Å constitute an interesting tool to infer the magnetic field

strength (e.g. Berdyugina & Fluri 2004; Milić & Faurobert 2012). Nevertheless, some discrepancies have been found in the results regarding magnetic field strengths (e.g. Asensio Ramos & Trujillo Bueno 2005; Derouich et al. 2006; Kleint et al. 2010). To eliminate a primary cause of these discrepancies, the effect of collisions in the formation of molecular lines should be taken into account. In fact, the main difficulty facing all Hanle diagnostics of the molecular lines is that collisional rates are poorly known. Particularly, collisions with hydrogen atom are of great importance due to its high density in the photosphere where Hanle effect is in action. Ignoring collisions has a significant consequence on the precise determination of magnetic fields, as collisions compete with the Hanle depolarizing effect of the turbulent photospheric magnetic fields. To contribute in addressing this difficulty, Qutub et al. (2020, 2021) calculated, for the first time, the collisional depolarization and polarization transfer rates of the ground states of the MgH and CN molecules by collisions with hydrogen atoms. In a contin-

uation of this effort, we aim to compute the depolarization and transfer of polarization rates for the two lowest energy electronic states of C<sub>2</sub> due to collisions with hydrogen atoms.

As C<sub>2</sub> is a homonuclear molecule, transitions between rotational levels with different parities cannot occur (see e.g. Flower 1990; Derouich 2006). This restriction arises from the symmetry of the interaction potential. However, this does not imply that C<sub>2</sub> molecule is immune to collisions. As it will be demonstrated through this paper, collisional transitions between rotational levels with same parity can affect the polarization of the C<sub>2</sub> electronic levels, and, therefore affect the polarization of the C<sub>2</sub> solar lines (e.g. Kleint et al. 2010). In this regard, we calculate the depolarization and polarization transfer rates of the solar C<sub>2</sub> molecules in their ground and first excited states  $X^1\Sigma_g^+$  and  $a^3\Pi_u$  due to collisions with H atoms in their ground state  $^2S_{1/2}$ .

The first step of this calculation is the determination of potential energy surfaces (PESs) for H+C<sub>2</sub> interactions. All the PESs are obtained using the MOLPRO package (e.g. Werner et al. 2010). The second step is the determination of the dynamics of collisions by solving the corresponding Schrödinger equations. The dynamics calculations are made possible thanks to the MOLSCAT code (e.g. Hutson & Green 1994). Then, the depolarization and polarization transfer cross-sections are computed within the tensorial basis  $T_q^k$  where  $k$  is the tensorial order and  $q$  quantifies the coherence within the molecular level. Note that these cross-sections are  $q$ -independent since the collisions are isotropic. We adopt the infinite order sudden (IOS) approximation to calculate the cross-sections for kinetic energies ranging from 50 to 40,000 cm<sup>-1</sup> allowing the calculation of depolarization and polarization transfer rates for temperatures ranging from  $T=2,000$  to 15,000 K. Finally, genetic programming methods are applied to infer useful analytical expressions of the obtained rates. In addition, the expected solar implications of our results are briefly discussed. Our cross sections are available online for future use by the community.

## 2. Potential Energy Surfaces

We consider the ground  $X^1\Sigma_g^+$  and the first excited  $a^3\Pi_u$  electronic states of C<sub>2</sub> molecule which are close in energy with spacing between the two states of about only 700 cm<sup>-1</sup> (i.e.  $\sim 0.087$  eV) (see e.g. Martin 1992). When C<sub>2</sub> ( $X^1\Sigma_g^+$ ) interacts with the hydrogen atom H in its  $^2S$  ground electronic state, the resultant system can exist in one electronic state  $1^2A'$ . Furthermore,  $2^2A'$  and  $2^2A''$  represent the two states which result from the interaction between C<sub>2</sub>( $a^3\Pi_u$ ) and H ( $^2S$ ). We adopt the coordinate system of Jacobi ( $R, r_{C_2}, \theta$ ) for the calculation of the PESs. The intermolecular vector  $R$  connects the center of mass of C<sub>2</sub> molecule and the hydrogen atom. The angle  $\theta$  defines the rotation of the hydrogen atom around the C<sub>2</sub> molecule. In the present work, the C<sub>2</sub> molecule is assumed to be rigid rotor with C-C distance frozen at its equilibrium value  $r_{C_2} = 2.348 a_0$  (Huber & Herzberg 1979). This is justified in the solar physical conditions where the rates for vibrational excitations due to collisions are much smaller than those for pure rotational excitations.

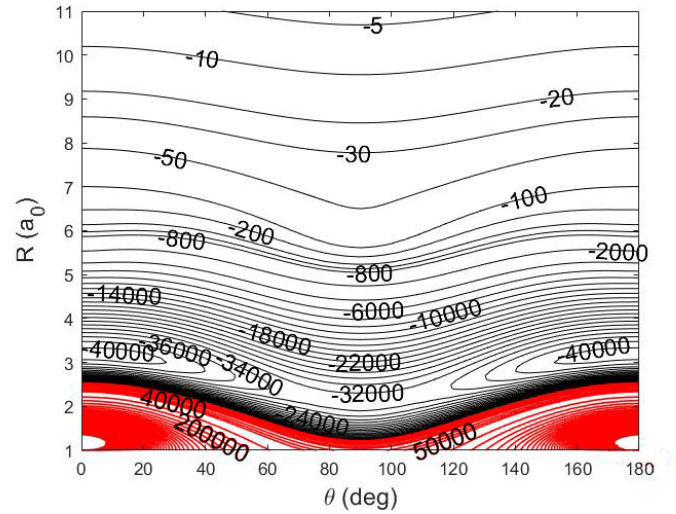


**Fig. 1.** Contour plot of the PES of the electronic state  $1^2A'$  as a function of  $R$  and  $\theta$ . Energy is in cm<sup>-1</sup>.

Ab initio calculations of the PESs for the electronic states of C<sub>2</sub>-H system, described above, were carried out using the multi-reference configuration interaction wave functions including Davidson correction (MRCI+Q) (see Langhoff & Davidson 1974; Davidson & Silver 1977; Werner & Meyer 1981; Wener & Knowles 1988). The computations were performed using the MOLPRO 2010 package (e.g. Werner et al. 2010).

For the electronic states under consideration, the two dimensional PESs were generated for an angle  $\theta$  ranging from 0 to 90° by using a variable step in order to well cover the behavior of the PESs and by varying the  $R$  values from  $a_0$  to 50  $a_0$ . We used 84 values of  $R$  ( $a_0 \leq R \leq 50 a_0$ ) and 51 values of  $\theta$  ( $0^\circ \leq \theta \leq 90^\circ$ ) implying that the total number of the generated ab initio points is 4284 for each potential surface  $V(R, \theta)$ . Note that, since C<sub>2</sub> is a homonuclear molecule, the interaction potential  $V$  is invariant under exchange of the two carbon atoms, i.e.,  $V(R, \theta) = V(R, 180^\circ - \theta)$ . The PES of the electronic state  $1^2A'$ , resulting from C<sub>2</sub> ( $X^1\Sigma_g^+$ ) and H ( $^2S$ ) interaction, is shown in Figure 1. Furthermore, PESs of the  $2^2A'$  and  $2^2A''$  states represented in the Figure 2 result from the interaction between C<sub>2</sub>( $a^3\Pi_u$ ) and H ( $^2S$ ).

The PES corresponding to the state  $1^2A'$  reaches its minimum at  $R \sim 3.2 a_0$  and  $\theta \sim 0^\circ$ , with an energy of  $E \sim -41,000$  cm<sup>-1</sup>. The PESs corresponding to the state  $2^2A'$  and  $2^2A''$  states have a similar minimal energy  $E \sim -39,000$  cm<sup>-1</sup> with  $\theta \sim 0^\circ$  and  $R \sim 3.2 a_0$ .

## 3. Collisional problem

In the context of the close coupling (CC) scheme, generating comprehensive results for depolarization and polarization transfer rates of the C<sub>2</sub> molecule is very difficult given the numerous rotational levels, the spin characteristics, and the large number of possible  $k$ -values for each rotational level. To overcome this difficulty we adopt the IOS approximation, which is appropriate for solar temperatures, to treat the collision prob-

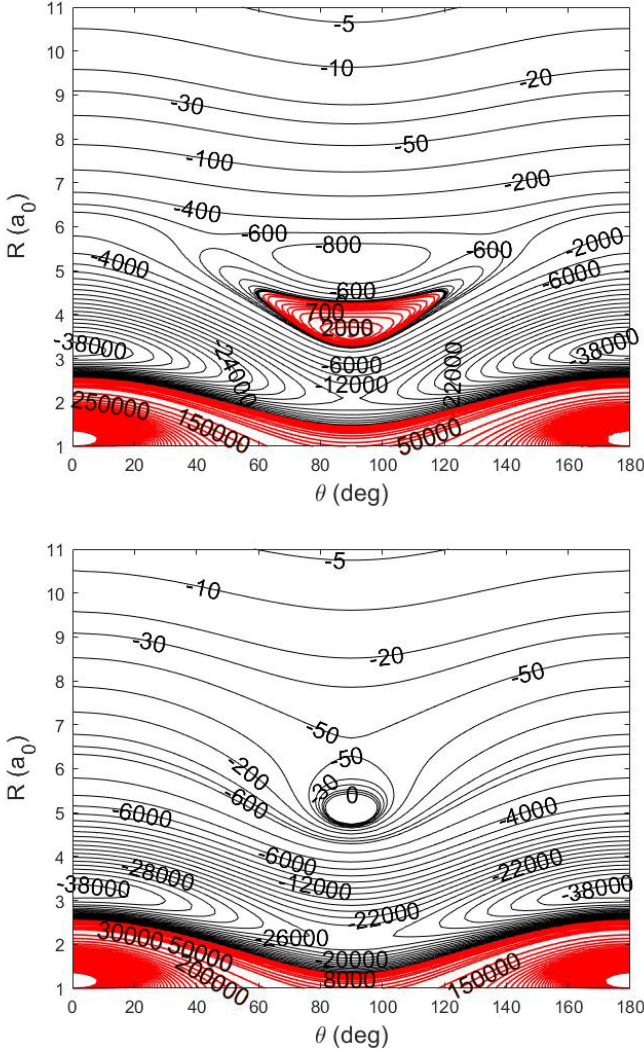


**Fig. 2.** Contour plots of the PESs of the electronic states  $2^2A'$  (upper panel) and  $2^2A''$  (lower panel) as functions of  $R$  and  $\theta$ . Energy is in  $\text{cm}^{-1}$ .

lem and provide a comprehensive data for all collisional rates. As we are interested in the solar context, where the temperature and the kinetic energies of collisions are sufficiently high, one can expect that some simplification regarding the coupling effects should be invoked in order to obtain results with acceptable accuracy in a reasonable calculation time.

We adopt a formalism developed by Corey & Alexander (1985) which is based on the decoupling of the rotational-orbital motion from the atomic and molecular spin angular momenta (see also Corey & McCourt 1983). This decoupling scheme offers an advantage in our attempt to express the tensorial cross-sections in terms of the generalized IOS cross-sections especially for the case of  $\text{C}_2(a^3\Pi_u)$  state where the orbital angular momentum and the spin of the molecule are non-zero. It is worth mentioning that, in a collision between an open-shell molecule (like  $\text{C}_2 a^3\Pi_u$ ) and an open-shell target (like  $\text{H } 2^2S$ ) the PESs is dependent of the total spin of the composite atom-molecule system and that dependence is taken into account in the PESs calculations. However, we neglect the

effect of the spin of the hydrogen in the dynamics of collisions and we only take into account the molecular spin which is a further approximation necessary for expressing the tensorial cross-sections factorized into products of terms involving the IOS cross-sections. In these conditions, one has (see Equations 13a,b,c of Corey & Alexander 1985):

$$\begin{aligned} \mathbf{N} &= \mathcal{R} + \mathbf{L} \\ \mathbf{j} &= \mathbf{N} + \mathbf{S}_d \end{aligned} \quad (1)$$

where  $\mathcal{R}$  is the rotational angular momentum of the diatomic  $\text{C}_2$  molecule and  $\mathbf{S}_d$  its spin;  $S_d = 0$  for  $X^1\Sigma_g^+$  and  $S_d = 1$  for  $a^3\Pi_u$ .  $\mathbf{L}$  is the electronic orbital momentum of the molecular state;  $L = 0$  for  $X^1\Sigma_g^+$  and  $L = 1$  for  $a^3\Pi_u$ . Note that  $\mathbf{N}$  is the total rotational-orbital angular momentum and  $\mathbf{j}$  is the total momentum of the molecule taking into account the spin.

In the framework of the coupling scheme given in Equation (1) and by following a methodology similar to that explained in different works concerned with molecule-atom collisions and by including the IOS approximation (e.g. Pack 1972, 1974; Alexander & Davis 1983; Alexander & Dagdigian 1983; Corey & Alexander 1985, 1986; Corey & Smith 1985; Werner, et al. 1989; Follmeg et al. 1990; Green 1994; Dagdigian & Alexander 2009 a,b,c; Paterson et al. 2009; McGurk et al. 2012), one can show that:

$$\begin{aligned} \sigma_{IOS}^k(el, j \rightarrow j', E) &= \sum_K (-1)^{k+j+j'+K} (2\mathcal{R} + 1)(2\mathcal{R}' + 1) \\ &\quad (2j' + 1)(2j + 1)(2N + 1)(2N' + 1) \\ &\quad \left\{ \begin{matrix} j & j' & K \\ j' & j & k \end{matrix} \right\} \left\{ \begin{matrix} \mathcal{R} & \mathcal{R}' & K \\ N' & N & L \end{matrix} \right\}^2 \\ &\quad \left\{ \begin{matrix} N & N' & K \\ j' & j & S_d \end{matrix} \right\}^2 \left( \begin{matrix} \mathcal{R}' & \mathcal{R} & K \\ 0 & 0 & 0 \end{matrix} \right)^2 \sigma(el, 0 \rightarrow K, E) \quad , \end{aligned} \quad (2)$$

where  $E$  is the kinetic energy and  $\sigma_{IOS}^k(el, j \rightarrow j', E)$  are the IOS polarization transfer cross sections from the level  $(\mathcal{R}Nj)$  to  $(\mathcal{R}'N'j')$  within the electronic state  $el$  and  $\sigma(el, 0 \rightarrow K, E)$  are the generalized IOS cross-sections. From the general formula of Equation (2), one can recover the limiting case where  $S_d = L = 0$  (see e.g. Derouich 2006; Lique et al. 2007).

The depolarization cross-section of the level  $(\mathcal{R}Nj)$  is given by:

$$\sigma_{IOS}^k(el, j, E) = \sigma_{IOS}^0(el, j \rightarrow j, E) - \sigma_{IOS}^k(el, j \rightarrow j, E) \quad , \quad (3)$$

where  $\sigma_{IOS}^k(el, j \rightarrow j, E)$  is obtained from Equation (2) with  $j = j'$ ,  $\mathcal{R} = \mathcal{R}'$ , and  $N = N'$ .

For the resolution of the collision dynamics of the problem at hand under the IOS approximation, the PESs were introduced into the MOLSCAT code (e.g. Hutson & Green 1994). As a result, we obtain the generalized IOS cross-sections  $\sigma(el, 0 \rightarrow K, E)$  for energies  $50 \leq E \text{ (cm}^{-1}\text{)} \leq 40,000$  and  $0 \leq K \leq 158$  ( $K$  is even). The data giving  $\sigma(el, 0 \rightarrow K, E)$  for all  $E$  and  $K$  values and for  $el = a^3\Pi_u$  and  $el = X^1\Sigma_g^+$  are made accessible online<sup>1</sup>. For each PES we obtain an IOS cross-section  $\sigma(el, 0 \rightarrow K, E)$ , so that we obtain  $\sigma(1^2A', 0 \rightarrow$

<sup>1</sup> Our IOS data are provided to enable reproduction of the IOS rates.

$K, E$ ) for the PES corresponding to the  $1^2A'$  state resulting from C<sub>2</sub> ( $X^1\Sigma_g^+$ ) and H ( $^2S$ ) interaction, i.e.,

$$\sigma(\text{el} = X^1\Sigma_g^+, 0 \rightarrow K, E) = \sigma(1^2A', 0 \rightarrow K, E), \quad (4)$$

while  $\sigma(2^2A', 0 \rightarrow K, E)$  and  $\sigma(2^2A'', 0 \rightarrow K, E)$  are obtained by solving the collision dynamics after introducing the PESs of the  $2^2A'$  and  $2^2A''$  states, respectively. The  $2^2A'$  and  $2^2A''$  result from the interaction between C<sub>2</sub>( $a^3\Pi_u$ ) and H ( $^2S$ ) and have the same spin. Thus, in order to obtain the cross-section corresponding to the C<sub>2</sub>( $a^3\Pi_u$ ) + H ( $^2S$ ) one has:

$$\begin{aligned} & \sigma(\text{el} = a^3\Pi_u, 0 \rightarrow K, E) \\ &= \frac{\sigma(2^2A', 0 \rightarrow K, E) + \sigma(2^2A'', 0 \rightarrow K, E)}{2}. \end{aligned} \quad (5)$$

The  $\sigma_{IOS}^k(\text{el}, j \rightarrow j', E)$  are then obtained by applying Equation (2). The depolarization rates

$$D^k(\text{el}, j, T) = D^0(\text{el}, j \rightarrow j) - D^k(\text{el}, j \rightarrow j) \quad (6)$$

of the level ( $\mathcal{R}Nj$ ) due to elastic collisions and the polarization transfer rates  $D^k(\text{el}, j \rightarrow j', T)$  between the levels ( $\mathcal{R}Nj$ ) and ( $\mathcal{R}'N'j'$ ) due to inelastic collisions are obtained by thermally averaging the respective IOS cross-sections:

$$\begin{aligned} D^k(\text{el}, j \rightarrow j', T) &= n_H \langle \sigma_{IOS}^k(\text{el}, j \rightarrow j', E) v \rangle \\ &= n_H \left( \frac{8k_B T}{\pi \mu} \right)^{\frac{1}{2}} \int_0^\infty \sigma^k(\text{el}, j \rightarrow j', \epsilon) e^{-\epsilon} \epsilon d\epsilon \end{aligned} \quad (7)$$

for temperatures in the range 2,000–15,000 K. Here  $n_H$  is the density of the incident hydrogen atoms,  $k_B$  is the Boltzmann constant, and  $\epsilon = E/k_B T$ .

In the case of homonuclear molecules like C<sub>2</sub>, collisional transitions between levels with even and odd  $j$ -values (or  $\mathcal{R}$ -values in the considered decoupling scheme) cannot occur (see e.g. Flower 1990; Derouich 2006). This fact is related to the symmetry of the interaction potential where  $V(R, \theta) = V(R, 180^\circ - \theta)$  (see Section 2). But obviously, this does not mean that the C<sub>2</sub> molecule is immune to collisions. Collisional transitions with  $\Delta j$  (or  $\Delta \mathcal{R}$  in our case) even are allowed which constitute a possibility of a collisional contribution to the statistical equilibrium equations (SEE) given by:

$$\begin{aligned} \left( \frac{d^j \rho_q^k}{dt} \right)_{coll} &= -[D^k(j, T) \\ &+ \sum_{j' \neq j} \sqrt{\frac{2j'+1}{2j+1}} D^0(j \rightarrow j', T)]^j \rho_q^k \\ &+ \sum_{j' \neq j} D^k(j' \rightarrow j, T) j' \rho_q^k, \end{aligned} \quad (8)$$

where  $j \rho_q^k$  are the density matrix elements expressed in the tensorial basis which permit a description of the internal states of the C<sub>2</sub> molecule (e.g. Sahal-Br  chot 1977; Landi Degl'Innocenti & Landolfi 2004). The importance of the collisional effects is mainly associated with the value of  $n_H$  and, to a lesser extent, with  $T$ . In the case of isotropic collisions, transfer of polarization rates obey the detailed balance relation:

$$D^k(j \rightarrow j', T) = \frac{2j'+1}{2j+1} \exp\left(\frac{E_j - E_{j'}}{k_B T}\right) D^k(j' \rightarrow j, T) \quad (9)$$

where  $E_j$  is the energy of the level ( $j$ ).

## 4. Results

We have determined polarization transfer rates  $D^k(j \rightarrow j', T)$  and depolarization rates  $D^k(j, T)$  associated to rotational levels within C<sub>2</sub> electronic states  $X^1\Sigma_g^+$  and  $a^3\Pi_u$ . When possible, genetic programming (GP) fitting techniques were employed to express these rates as two-variable functions, with the variables being  $j$  which varies from 0 to 60 and  $T$  which goes from 2,000 to 15,000 K. The GP expression is:

$$D_{GP}^k = n_H \times 10^{-10} \frac{\sum_i a_i^k j^{\alpha_i^k} T^{\beta_i^k}}{\sum_i b_i^k j^{\gamma_i^k} T^{\delta_i^k}}, \quad (10)$$

where the GP coefficients  $a_i^k$ ,  $\alpha_i^k$ ,  $\beta_i^k$ ,  $b_i^k$ ,  $\gamma_i^k$ , and  $\delta_i^k$  are provided in Tables A.1–A.6 of the Appendix A. As representative examples, we provide  $D^k(j \rightarrow j', T)$  and  $D^k(j, T)$  for 6 cases. However, Equation 2 can be used to derive any other case by incorporating the quantum numbers of interest and summing over the generalized IOS cross-sections  $\sigma(0 \rightarrow K, E)$ , conveniently accessible online. Once cross-sections are obtained one should perform an average over the energies to obtain the rates (see Equation (7)). This enables non-specialized readers to obtain cross-sections/collisional rates for any C<sub>2</sub> rotational level within the electronic states  $X^1\Sigma_g^+$  and  $a^3\Pi_u$ .

### 4.1. Results for $X^1\Sigma_g^+$ -state

Figure 3 shows the variation of the collisional depolarization rates  $D^k(j, T)$  for the alignment ( $k=2$ ) and orientation ( $k=1$ ) as functions of  $j$  at  $T = 6,000$  K in the upper panel and as functions of  $T$  for the level  $N_j = 6_6$  in the lower panel. The depolarization rates with tensorial order  $k=2$  are larger than those with tensorial order  $k=1$ , as seen in Figure 3. As one would expect, the  $D^k(j, T)$  rates increase with temperature (for a given  $j$ ) and decrease with increasing  $j$  (for a given  $T$ ) (see e.g. Derouich 2006). The  $D_{GP}^k(j, T)$  rates determined by Equation (10) and Table A.1 are shown by the solid curves in Figure 3, and they show excellent agreement with the  $D^k(j, T)$  rates that were computed directly. The percentage error on the  $D_{GP}^k(j, T)$  values is less than 5% for any  $j$  and  $T$  in the considered ranges.

In the upper panel of Figure 4, we set  $\Delta j = j' - j = 2$  and  $T = 6,000$  K and we show the dependence of the excitation (i.e.  $E_{j'} > E_j$ ) transfer of polarization rates  $D^k(j \rightarrow j', T)$  for  $k=0$ ,  $k=1$ , and  $k=2$  as functions of  $j$ . The solid curves in the upper panel of Figure 4 show the excellent agreement between the real values calculated directly and the GP fit values obtained using Equation (10) and Table A.2. The percentage of difference between the real calculated values and the GP values is less than 5%. As it is shown in the upper panel of Figure 4, the  $D^k(j \rightarrow j' = j+2, T)$  rapidly increase with  $j$  for low values of  $j$  and vary slowly for sufficiently large  $j$ .  $D^k(j \rightarrow j' = j+2, T)$  can be considered practically constant for sufficiently large  $j$  values. We show in the lower panel of Figure 4 how the rates  $D^k(j \rightarrow j', T)$  decrease quickly with increasing of  $j' - j$  for the level  $N_j = 6_6$  and  $T = 6,000$  K.

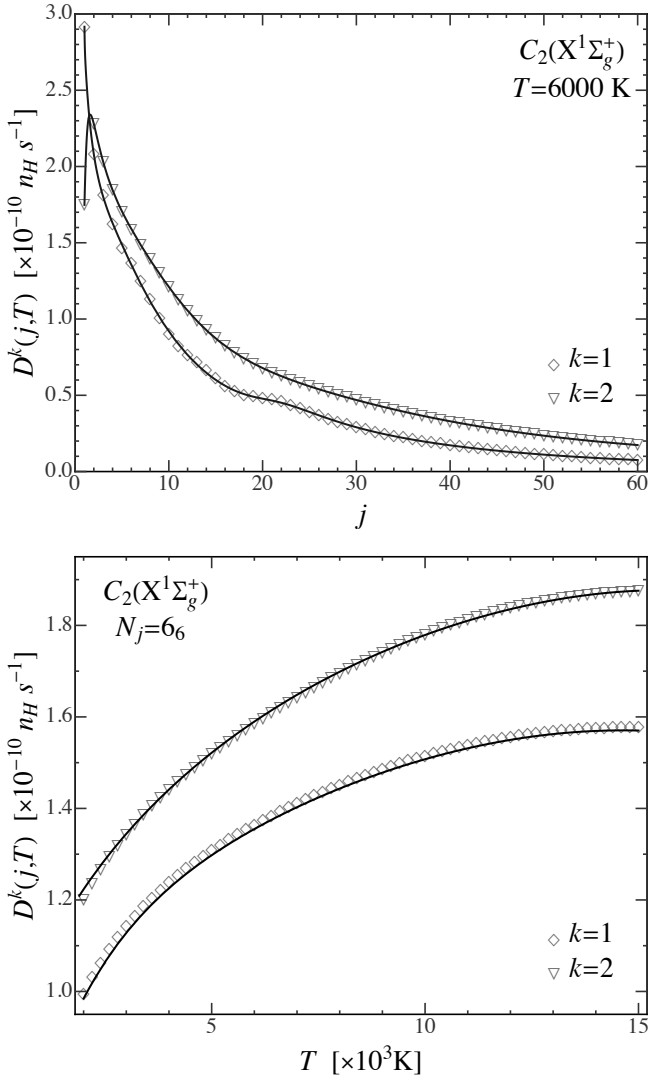


**Fig. 3.** Collisional depolarization rates,  $D^k(j, T)$ , for C<sub>2</sub> rotational levels within the electronic states  $X^1\Sigma_g^+$ . The variation of the rates with  $j$  (upper panel) and with  $T$  (lower panel) are shown for  $k = 1$  (open diamonds) and  $k = 2$  (open triangles). The solid curves show the GP fit values obtained using Equation (10) and Table A.1.

#### 4.2. Results for a $^3\Pi_u$ -state

For the electronic state  $a^3\Pi_u$ , with molecular spin  $S_d = 1$ ,  $j$  can take values of  $N - 1$ ,  $N$ , or  $N + 1$ . As illustrated in the upper panel of Figure 5, for  $j \gtrsim 5$  the depolarization rates,  $D^k(j, T)$ , decrease with increasing  $j$  for constant temperature. Additionally, the depolarization rates increase as  $T$  increases for constant  $j$  as it can be seen in the lower panel of Figure 5. We note that the depolarization rates with tensorial order  $k = 2$  are larger than those with tensorial order  $k = 1$ . This is also the case for the state  $X^1\Sigma_g^+$ . By using GP fitting techniques, analytical expressions for  $D^k(j, T)$  rates were obtained. These are given by Equation (10) in the temperature range 2,000 – 15,000 K and for total angular momentum  $j$  going from 1 to 60 with the GP coefficients provided in Tables A.3, A.4 and A.5

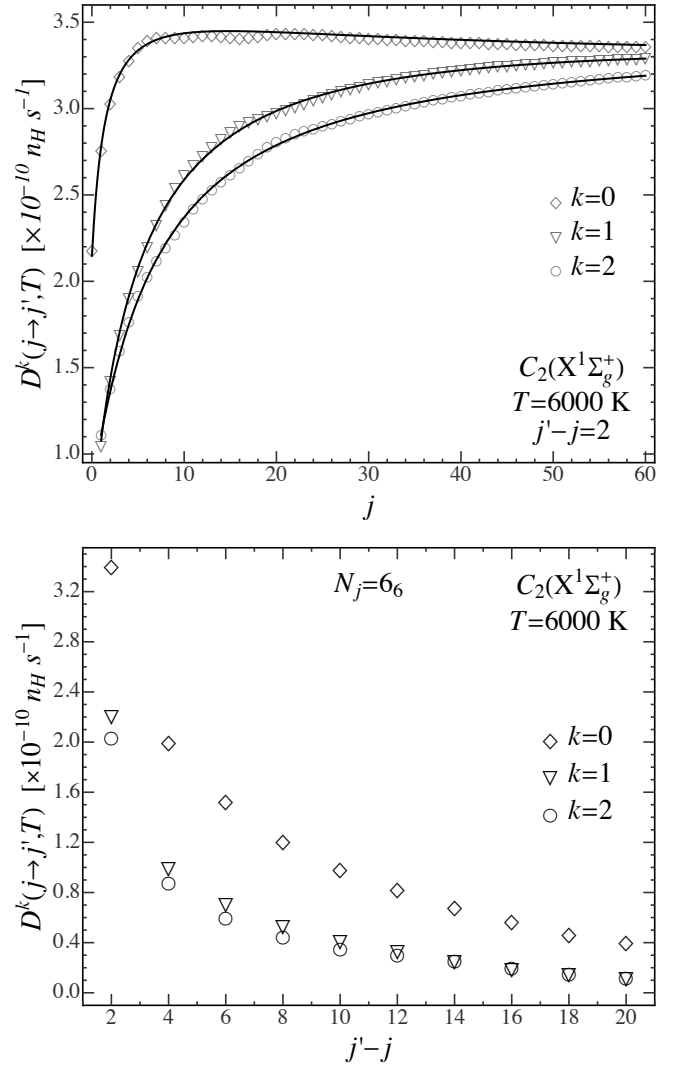


**Fig. 4.** Collisional transfer rates,  $D^k(j \rightarrow j', T)$ , for C<sub>2</sub> rotational levels within the electronic states  $X^1\Sigma_g^+$ . The variation of the rates for  $k = 0$  (open diamonds),  $k = 1$  (open triangles), and  $k = 2$  (open circles) are shown in the upper panel as functions of  $j$  for  $j' - j = 2$  and  $T = 6,000$  K and as functions of  $j' - j$  for the level  $N_j = 6_6$  and  $T = 6,000$  K in the lower panel. The solid curves in the upper panel show the GP fit values obtained using Equation (10) and Table A.2.

for  $j = N - 1$ ,  $j = N$  and  $j = N + 1$ , respectively. The percentage error in the GP rates  $D_{GP}^k(j, T)$  are less than 5%.

Figure 6 shows the rates of polarization transfer associated with C<sub>2</sub> rotational levels within the electronic states  $a^3\Pi_u$ . The upper panel of Figure 6 illustrates significant increase in the transfer rates  $D^k(j \rightarrow j' = j + 2, T)$  as  $j$  increases for sufficiently small  $j$ . For  $j \gtrsim 20$ , the transfer rates keep increasing with increasing  $j$  but rather slowly. This result gives interesting insights on the differential effect of collisions when comparing the polarization of molecular lines with different  $j$ -values. In fact, for lines involving levels with sufficiently large  $j$ , the  $D^k(j \rightarrow j' = j + 2, T)$  can be considered practically constant

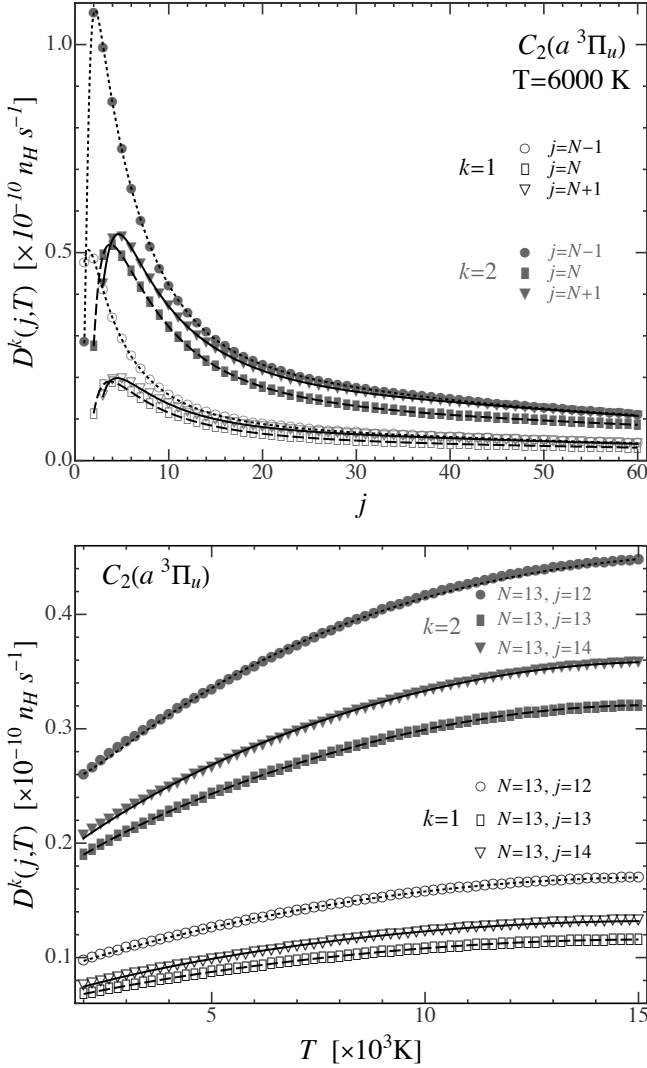


**Fig. 5.** Collisional depolarization rates,  $D^k(j, T)$ , for C<sub>2</sub> rotational levels in electronic states  $a^3\Pi_u$ . The upper panel illustrates the rates for  $k=1$  (open markers) and  $k=2$  (solid markers) with respect to  $j$  at  $T=6,000$  K, where  $j=N-1$  (circles),  $j=N$  (rectangles), and  $j=N+1$  (triangles) are displayed. The lower panel shows the temperature variation of the rates for  $k=1$  (open markers) and  $k=2$  (solid markers) with the different  $j$  values of the  $N=13$  multiplet. Both panels display fitted values (dotted, dashed, and solid curves) obtained using Equation (10) and GP coefficients of Tables A.3, A.4, and A.5.

which greatly simplify the modeling. This is also the case for the electronic state  $X^1\Sigma_g^+$ .

## 5. Why use IOS approach in the collision dynamics?

Unlike close-coupling (CC) methods, which are both time-intensive and require case-by-case calculations, the IOS approach allows for the derivation of comprehensive tables containing generalized IOS cross-sections. These tables facilitate the efficient generation of collisional rates for all transitions

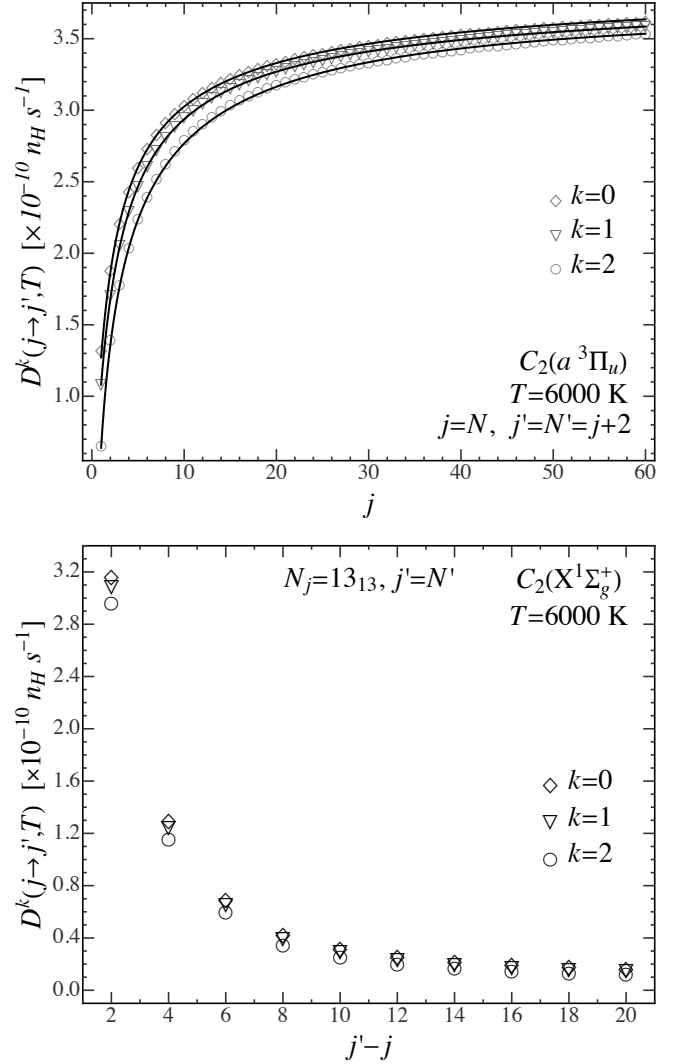


**Fig. 6.** Collisional transfer rates,  $D^k(j \rightarrow j', T)$ , for C<sub>2</sub> rotational levels within the electronic states  $a^3\Pi_u$ . The upper panel shows variation with  $j$  of the rates for  $k=0$  (open diamonds),  $k=1$  (open triangle), and  $k=2$  (open circles) where we have set  $j'-j=2$  and  $T=6,000$  K. The solid curves show the GP fit values obtained using Equations (10) and GP coefficients of Table A.6. The lower panel displays the variation of the rates with  $j'-j$  for  $k=0$  (open diamonds),  $k=1$  (open triangle), and  $k=2$  (open circles) where we set  $T=6,000$  K,  $N_j=13_{13}$ , and  $j'=N'$ .

and tensorial orders  $k$ , with good accuracy, particularly at solar temperatures ( $T > 5000$  K).

To assess the validity of the IOS approximation, we carry out a CC calculation of cross sections using the PES of the interaction  $C_2(X^1\Sigma_g^+) + H^2S$  for kinetic energies upto  $5000 \text{ cm}^{-1}$  which allows the calculation of collisional rates upto  $1300 \text{ K}$  with accuracy better than few percent. In Figure 7, we compare the IOS rate to CC rate for the collisional rotation transition  $j=6 \rightarrow j'=4$ . The IOS collisional rate, which is smaller for low temperatures, converges to the CC collisional rate as temperature increases; the difference between the two

rates becomes less than 5% for  $T = 1300$  K (see Figure 7). For higher temperatures, in particular solar temperature, the difference should be negligibly small. This should also hold true for the PESs arising from interaction between C<sub>2</sub>( $a^3\Pi_u$ ) and H( $^2S$ ).

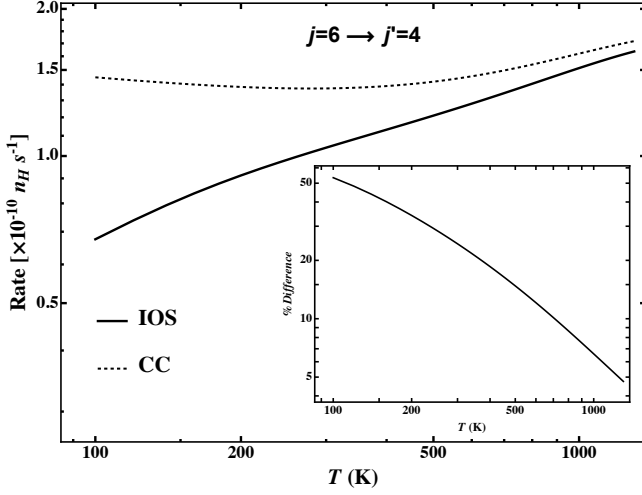


**Fig. 7.** Comparison between the IOS rate (solid curve) and the CC rate (dashed curve) for the collisional rotational de-excitation,  $j=6 \rightarrow j'=4$  as functions of temperature. In addition, an inset figure is provided to focus on the % difference between the two rates. The % difference  $|\frac{CCrate-IOSrate}{CCrate}| \times 100$  drops to less than 5% at  $T = 1300$  K.

We also compare our IOS collisional rotational de-excitation cross sections, obtained with our PES for C<sub>2</sub>( $X^1\Sigma_g^+$ ) + H( $^2S$ ), to the corresponding coupled-state cross sections of Najjar et al. (2014), calculated using their own PES. In particular, at an energy of approximately  $350$  cm<sup>-1</sup>, we find:

- For the transition  $j = 2 \rightarrow j' = 0$ , our cross section is  $1.53 \text{ \AA}^2$ , while the cross section of Najjar *et al.* (2014) is  $2 \text{ \AA}^2$ .
- For  $j = 4 \rightarrow j' = 0$ , our cross section is  $0.75 \text{ \AA}^2$ , while the cross section of Najjar *et al.* (2014) is  $0.8 \text{ \AA}^2$ .

The differences are smaller than 25% at these relatively low energies and are expected to become negligible for the higher energies that contribute to the rates at temperatures above 2000 K, which are the focus of this paper. It should be noted that Najjar *et al.* (2014) did not consider energies above  $350$  cm<sup>-1</sup>, and therefore, a comparison at higher energies is not possible.

## 6. Solar implications

Observations of the second solar spectrum (SSS) revealed the existence of prominent linear polarization signals due to lines of the C<sub>2</sub> molecule (e.g. Gandorfer 2000; Faurobert & Arnaud 2003; Gandorfer et al. 2004; Kleint et al. 2008). Further, theoretical analyses pointed out the suitability of these lines for the application of the differential Hanle effect to study variations of turbulent magnetic fields in the photosphere where

C<sub>2</sub> lines region around  $5141 \text{ \AA}$  form (e.g. Berdyugina & Fluri 2004; Kleint et al. 2010; Kleint et al. 2011; Milić & Faurobert 2012). Nevertheless, such theoretical studies faced the problem of the total lack of collisional rates which impacted the accuracy of their conclusions.

We consider the implication of our results for the molecular C<sub>2</sub> lines of the Swan system ( $d^3\Pi_u - a^3\Pi_u$ ). In particular, we select the triplet R<sub>1</sub>(14), R<sub>2</sub>(13) and R<sub>3</sub>(12) of the R-branch and the P-triplet P<sub>1</sub>(42), P<sub>2</sub>(41), P<sub>3</sub>(40) which are suitable for solar magnetic field diagnostics (see Kleint et al. 2010). To estimate the effect of isotropic collisions, we compare the collisional depolarization rates  $D^2(j, T)$  of the lower state  $a^3\Pi_u$  for typical photospheric hydrogen density ( $n_H = 10^{15} - 10^{16} \text{ cm}^{-3}$ ), to the inverse lifetime ( $1/t_{\text{life}} = B_{\ell u} I(\lambda_{\ell u})$ ) of the lower levels of the R-triplet and P-triplet lines. Here  $I(\lambda_{\ell u})$  denotes the intensity of light of wavelength  $\lambda_{\ell u}$  at the center of the solar disk incident on the C<sub>2</sub> molecules, and  $B_{\ell u} = (w_u/w_\ell)(c^2/2h\nu_{u\ell}^3)A_{u\ell}$  denotes the Einstein coefficient for absorption with  $A_{u\ell}$  being the transition probability per unit time for spontaneous emission,  $\nu_{u\ell}$  the line frequency,  $w_u$  and  $w_\ell$  the statistical weights of upper and lower levels,  $h$  the Planck's constant, and  $c$  the speed of light. We note that the rate of radiative relaxation from the electronic state  $a^3\Pi_u$  to the lower energy electronic state  $X^1\Sigma_g^+$  is negligibly small (see e.g. Wehres et al. 2010).

In Table 1, we show  $B_{\ell u} I(\lambda)$  and the linear depolarization rates,  $D^{k=2}(j_\ell)$ , calculated at the effective photospheric temperature,  $T_{\text{eff}} = 5778$  K, and at typical values of Hydrogen density  $n_H = 10^{15} \text{ cm}^{-3}$  and  $n_H = 10^{16} \text{ cm}^{-3}$  in the photosphere. The values of the core relative intensity of the absorption lines are taken from the solar atlas of Delbouille et al. (1972) whereas the corresponding absolute continuum values are interpolated from the data given in Allen (1976). The values of the Einstein  $A_{u\ell}$  coefficients are derived from Kleint et al. (2010).

In the case of the R-triplet, the linear depolarization rates  $D^{k=2}$  are roughly  $\frac{1}{3}B_{\ell u} I(\lambda_{\ell u})$  for  $n_H = 10^{15} \text{ cm}^{-3}$  which means that the lower levels of the R-triplet lines residing within the electronic state C<sub>2</sub>  $a^3\Pi_u$  should be affected by the depolarizing collisions. On the other hand, for  $n_H = 10^{16} \text{ cm}^{-3}$ , the linear depolarization rates  $D^{k=2}$  of the lower levels for lines of the R-triplet are roughly  $3 B_{\ell u} I(\lambda_{\ell u})$  which renders the depolarizing effect of collisions stronger. Nevertheless, for both perturbers' densities the depolarizing collisional rates are not sufficiently high to completely depolarize the lower levels of the R-triplet lines.

Similarly for the P-triplet case in the typical photospheric conditions, the lower levels for lines of the triplet cannot be completely depolarized by collisions given that the collisional depolarization rates  $D^{k=2}$  of these levels, which are relatively lower given the relatively larger  $j$  values (see the upper panel of Figure 5), are comparable to their inverse lifetime,  $B_{\ell u} I(\lambda_{\ell u})$ , (see Table 1).

It is clear that with the typical photospheric densities,  $n_H = 10^{15} - 10^{16} \text{ cm}^{-3}$ , collisions with hydrogen atoms partially depolarize the rotational levels of the lower electronic level of the C<sub>2</sub> lines of the Swan system ( $d^3\Pi_u - a^3\Pi_u$ ). Hence, one has

to incorporate the collisional depolarization rates when solving the SEE for the polarization of observed lines.

The R-branch lines, R<sub>1</sub>(14), R<sub>2</sub>(13), and R<sub>3</sub>(12), are more significantly affected by collisions compared to the P-branch lines, P<sub>1</sub>(42), P<sub>2</sub>(41), and P<sub>3</sub>(40), because the latter have larger *j*-values. As demonstrated in the previous section, the collisional effect decreases as *j* increases.

## 7. Conclusion

This paper continues a series of investigations concerned with the collisional depolarization of spectral lines of solar molecules such as MgH, CN, and C<sub>2</sub>. In this study, we have computed the quantum collisional depolarization and polarization transfer rates for C<sub>2</sub> ( $X^1\Sigma^+g, a^3\Pi_u$ ) + H( $^2S1/2$ ) isotropic collisions. The computation involved calculating the potential energy surfaces (PESs) using the MOLPRO package, followed by solving the quantum dynamics using the MOLSCAT code. Sophisticated genetic programming techniques were employed to derive analytical expressions for the temperature and total molecular angular momentum dependencies of the collisional depolarization and polarization transfer rates. The results show that isotropic collisions with neutral hydrogen partially depolarize the lower state of C<sub>2</sub> lines, implying the limitations of neglecting lower-level polarization. Collisional depolarization and polarization transfer rates are a fundamental ingredient for interpreting C<sub>2</sub> polarization in terms of magnetic fields in the quiet regions of the Sun.

**Acknowledgements.** This research work was funded by Institutional Fund Projects under grant no. (IFPIP:772-130-1443). The authors gratefully acknowledge technical and financial support provided by the Ministry of Education and King Abdulaziz University, DSR, Jeddah, Saudi Arabia. We thank François Lique for his insightful discussion on molecular collision physics.

## References

- Alexander, M.H. & Davis, S.L., 1983, *J. Chem. Phys.*, 79, 227  
 Alexander, M. H. & Dagdigian, P. J. 1983, *J. Chem. Phys.*, 79, 302  
 Allen, C. W., 1976, *Astrophysical Quantities*, (3rd ed., London: Athlone)  
 Asensio Ramos, A. & Trujillo Bueno, J., 2005, *ApJ Letters*, 635, 109  
 Berdyugina, S.V. & Fluri, D., 2004, *A&A*, 417, 775  
 Berdyugina, S.V., Stenflo, J.O., & Gandorfer, A., 2002, *A&A*, 388, 1062-107  
 Corey, G.C., & McCourt, F.R., 1983, *J. Phys. Chem.*, 87,2723  
 Corey, G.C., 1984, *J. Chem. Phys.*, 81, 2678  
 Corey, G.C. & Alexander, M., 1985, *J. Chem. Phys.*, 83, 5060  
 Corey, G.C., & Smith, A.D., 1985, *J. Chem. Phys.*, 83, 5663  
 Corey, G.C., Alexander, M., & Dagdigian, P.J., 1986, *J. Chem. Phys.*, 84, 1547  
 Dagdigian, P. & Alexander, M., 2009a, *J. Chem. Phys.*, 130, 094303  
 Dagdigian, P., & Alexander, M., 2009b, *J. Chem. Phys.*, 130, 164315  
 Dagdigian, P. & Alexander, M., 2009c, *J. Chem. Phys.*, 130, 204304  
 Davidson, E.R. & Silver, D.W., 1977, *Chem. Phys. Lett.*, 52, 403  
 Derouich, M., 2006, *A&A*, 449, 1  
 Derouich, M., Bommier, V., Malherbe, J.M., & Landi Degl'Innocenti, E., 2006, *A&A*, 457, 1047  
 Delbouille, L., Neven, L., & Roland, G., 1972, *BASS2000 Solar Survey Archive*, [http://bass2000.obspm.fr/solar\\_spect.php](http://bass2000.obspm.fr/solar_spect.php)  
 Faurobert, M., & Arnaud, J., 2003, *A&A*, 412, 555  
 Flower, D., 1990, *Molecular Collisions in the Interstellar Medium* (Cambridge University Press: Cambridge)  
 Follmeg, B., Rosmus, P., & Werner, H.-J. 1990, *J. Chem. Phys.*, 93, 4687. doi:10.1063/1.458658  
 Gandorfer, A., 2000, *The Second Sol. Spectrum: A high spectral resolution polarimetric survey of scattering polarization at the solar limb in graphical representation*, Vol. 1: 4625 Å to 6995 Å (Hochschulverlag AG an der ETH Zurich)  
 Gandorfer, A.M., Steiner, H.P.P.P., Aebersold, F., et al., 2004, *A&A*, 422, 703  
 Green, S. 1994, *ApJ.*, 434, 188  
 Huber, K.P., & Herzberg, G. 1979, "Molecular Spectra and Molecular Structure: Constants of Diatomic Molecules". Van Nostrand Reinhold, New York  
 Hutson, J.M., & Green, S., MOLSCAT computer code, version 14 (1994) distributed by Collaborative Computational Project  
 Kleint, L., Berdyugina, S., & Bianda, M., 2008, *European Solar Physics Meeting*, 12, 2.71  
 Kleint, L., Berdyugina, S. V., Shapiro, A. I., Bianda, M., 2010, *A&A*, 524, A37  
 Kleint, L., Shapiro, A.I., Berdyugina, S.V., et al., 2011, *A&A*, 536, A47  
 Najjar, F., Ben Abdallah, D., Jaidane, N., 2014, *Chem. Phys. Lett.*, 608, 17  
 Landi Degl'Innocenti, E. & Landolfi, M. 2004, *Polarization in Spectral Lines* (Dordrecht: Kluwer)  
 Langhoff, S.R., & Davidson, E.R., 1974, *Int. J. Quantum Chem.* 8, 61  
 Lique, F., Spielfiedel, A., & Feautrier, N., 2007, *J. Phys. B: At. Mol. Phys.*, 40, 787  
 Martin, M. 1992, *J. Photochem. Photobiol. A: Chem.*, 66, 263  
 McGurk, S.J., McKendrick, K.G., Costen, M.L., Bennett, D.I.G., Klos, J., Alexander, M.H., & Dagdigian, P.J., 2012, *J. CHEM. PHYS.*, 136, 164306  
 Milić, I., & Faurobert, M., 2012, *A&A*, 547, id.A38, 7 pp.  
 Qutub, S., Derouich, M., Kalugina, Y.N., Asiri, H., & Lique, F., 2020, *MNRAS*, 491, 1213  
 Qutub, S., Kalugina, Y., & Derouich, M., 2021, *ApJ*, 915, 2, id.122, 6 pp  
 Pack, R.T., 1972, *Chem. Phys. Letters*, 14, 393  
 Pack, R.T., 1974, *J. Chem. Phys.*, 60, 633  
 Paterson, G., Marinakis, S., Costen M.L., & McKendrick, K.G., 2009, *Phys. Scr.* 80, 048111  
 Sahal-Bréchet, S., 1977, *ApJ*, 213, 887  
 Trujillo Bueno, J., Asensio Ramos, A., & Shchukina, N., 2006, *Solar Polarization 4 ASP Conference Series*, Vol. 358, R. Casini and B. W. Lites  
 Wehres, N., Romanzin, C., Linnartz, H., et al., 2010, *A&A*, 518, A36. doi:10.1051/0004-6361/201014475  
 Wiegelmann, T., Thalmann, J.K., & Solanki, S.K., 2014, *The magnetic field in the solar atmosphere. Astron. Astrophys. Rev.* 22, 78  
 Wöger, Friedrich, Rimmele, Thomas, Ferayorni, Andrew ; Beard, Andrew ; Gregory, Brian S. ; Sekulic, Predrag ; Hegwer, Steven L.  
 Werner, H.-J., & Meyer, W., 1981, *J. Chem. Phys.* 74, 5802  
 Werner, H.-J., Follmeg, B., Alexander, M.H., & Lemoine, D., 1989, *J. Chem. Phys.*, 91, 5425; doi: 10.1063/1.457570  
 Wener H.-J., Knowles P. J., 1988, *J. Chem. Phys.*, 89, 5803  
 Werner H.-J., Knowles P. J., Knizia G., Manby F. R., Schütz M. et al., MOLPRO, version 2010.1, a package of ab initio programs, 2010, see <http://www.molpro.ne>  
 Stenflo, J., 1994, *Solar Magnetic Fields: Polarized Radiation Diagnostics*, *Astrophys. Space Sci. Lib.* 189, Springer, Berlin



**Table 1.** Comparison between the linear depolarization rates  $D^2$  of the C<sub>2</sub>  $a^3\Pi_u$  state to its inverse lifetime  $1/t_{life}=B_{lu}I(\lambda)$ . Note that  $I(\lambda_{ul})$  is given in ( $10^{-5}\text{erg cm}^{-2}\text{s}^{-1}\text{sr}^{-1}\text{Hz}^{-1}$ ). The Lines are, respectively, R<sub>1</sub>(14), R<sub>2</sub>(13), R<sub>3</sub>(12), P<sub>1</sub>(42), P<sub>2</sub>(41) and P<sub>3</sub>(40).

$\lambda_{ul}$ (Å)	$j$	$I(\lambda_{ul})$	$B_{lu}I(\lambda_{ul})$ ( $10^5\text{s}^{-1}$ )	$D^2(j, T=5778\text{ K})$ ( $10^5\text{s}^{-1}$ )	
				$n_{\text{H}}=10^{15}\text{cm}^{-3}$	$n_{\text{H}}=10^{16}\text{cm}^{-3}$
5139.93	14	8.13008	0.845676	0.279154	2.79154
5140.14	13	8.62069	0.917542	0.253947	2.53947
5140.38	12	9.34579	1.014485	0.350343	3.50343
5141.21	42	8.26446	0.736174	0.136336	1.36336
5141.19	41	8.47458	0.754441	0.107232	1.07232
5141.31	40	8.69565	0.834171	0.145746	1.45746

## Appendix A: Different Tables giving the GP coefficients

**Table A.1.** GP coefficients corresponding to the analytical expression of Equation (10) for  $D^k(j = N, T)$ . Coefficients are given for both  $k = 1$  and  $k = 2$  for rotational levels of the  $\Sigma$ -state.

$i$	$a_i^k$	$\alpha_i^k$	$\beta_i^k$	$b_i^k$	$\gamma_i^k$	$\delta_i^k$
$k = 1$						
1	1.991191e-3	-0.581446	-0.3057279	2.775182e-8	4.8698780	-0.9948641
2	0.9256007	1.563707	-0.1573567	3.318555e3	0.7634837	-0.7735423
3	-0.9256059	1.563705	-0.1573564	-3.823419e3	0.7683499	-0.7727445
4	-1.272366e-4	1.524807	0.9668442	6.282801e2	0.8160999	-0.7646596
5	2.845039e-4	1.525127	0.9668662	-1.782060e2	0.9014560	-0.7490103
6	-1.572672e-4	1.525386	0.9668841	5.486061e1	0.9463913	-0.7401261
7	8.843118e-9	-35.64545	1.0808530	3.048508e-7	-1.8538130	0.9168674
8	2.461312e-8	-2.357598	1.3237760	1.441014e-21	-1.7989560	4.1172120
$k = 2$						
1	6.001485e-4	2.396011	0.5982441	-2.895777e-3	1.752254	0.8141479
2	-1.117526e-3	2.396003	0.5984454	2.895777e-3	1.752254	0.8141479
3	5.173784e-4	2.395994	0.5986782	2.718900e-14	4.056257	0.9387745
4	3.39671e-10	-0.5960658	1.464536	1.576906e-11	-1.520357	2.107281
5	1.659791e-9	-1.824684	2.816542	5.131261e-12	-5.888703	2.205830
6	-1.659459e-9	-1.824676	2.816558	7.264044e-35	-2.347249	7.450174

**Table A.2.** The GP coefficients, as per the analytical expression in Equation (10) for  $D^k(j = N \rightarrow j' = N + 2, T)$ , are provided for rotational levels of the  $\Sigma$ -state, where  $k = 0, 1$  and  $k = 2$ .

$i$	$a_i^k$	$j^{\alpha_i^k}$	$\beta_i^k$	$b_i^k$	$\gamma_i^k$	$\delta_i^k$
$k = 0$						
1	1.397544e3	1.184034	-1.020533	0.5188084	1.344210	2.070097e-2
2	7.100799e-2	1.598421	0.2540003	0.7106673	1.162418	0.1598386
3	3.735336e-2	0.9630494	0.7948434	4.799789e-2	0.8078731	0.5528220
4	-4.478655e-7	1.283280	1.599432	1.244310e-6	0.8860535	1.561604
5	5.633616e-2	0	0.7269272	0.4886689	0	0.3906900
$k = 1$						
1	-2.296152	0.7256945	-2.405169e-2	0.1039076	1.662413	0.3857427
2	3.809447e-2	1.475278	0.8186476	1.682204e-4	0.8653501	0.7800596
3	-1.193235e-2	1.261421	1.016065	-1.223617e-6	1.379011	1.540615
4	2.272656e-4	0.3249925	1.258974	1.693369e-5	0.6833434	1.551339
5	1.588990e-5	0.4005488	1.556258	2.137974e-5	-5.004082e-2	1.599273
6	3.827193e-5	1.063432	1.629335	6.390334e-9	1.267591	2.218129
$k = 2$						
1	-2.145054e-11	1.109234	2.934953	1.143386e-3	1.156976	0.9945199
2	1.144444e-2	0.9603254	0.9600221	9.317665e-4	1.333167	0.7144136
3	2.813450e-4	1.228673	1.047091	7.713058e-3	1.062634	0.7403552
4	1.605891e-5	1.219828	1.600001	3.864867e-3	0.9338449	0.8553057
5	5.890345e-2	0	0.8765076	1.064727	0	0.5685439

**Table A.3.** GP coefficients, corresponding to the Equation (10) for  $D^k(j = N - 1, T)$ , are provided for rotational levels within the  $\Pi$ -state, covering both  $k = 1$  and  $k = 2$ .

$i$	$a_i^k$	$j^{\alpha_i^k}$	$\beta_i^k$	$b_i^k$	$\gamma_i^k$	$\delta_i^k$
$k = 1$						
1	9.631358e-4	1.270850	0.9713363	3.821693e-7	0.477288	0.3895764
2	-1.529505e-3	1.271256	0.9713726	2.376594e-12	3.874105	0.6974655
3	5.663722e-4	1.271943	0.9714340	1.143000e-5	1.646778	1.556904
4	-3.359058e-5	0.5428953	1.523613	-1.142996e-5	1.646778	1.556904
5	3.359058e-5	0.5428957	1.523613	1.321659e-21	1.613181	3.739739
$k = 2$						
1	8.921348e-5	1.216925	1.193702	-1.536963e-2	1.063446	0.5335961
2	-2.910309e-4	1.198176	1.194265	1.532168e-2	1.062882	0.5342671
3	6.203630e-5	1.189519	1.194559	5.326371e-6	-4.183293	0.9498192
4	6.870049e-5	1.189240	1.194568	2.531897e-9	2.977568	0.9846094
5	7.120522e-5	1.189136	1.194572	5.741291e-14	1.042410	2.549029

**Table A.4.** GP coefficients, corresponding to the Equation (10) for  $D^k(j = N, T)$ , are presented for rotational levels within the  $\Pi$ -state, where  $k = 1$  and  $k = 2$ .

$i$	$a_i^k$	$j^{\alpha_i^k}$	$\beta_i^k$	$b_i^k$	$\gamma_i^k$	$\delta_i^k$
$k = 1$						
1	2.624783e-10	3.280700	0.7520319	0.2436235	1.459148	0.2180211
2	7.484584e-4	0.3670139	1.120077	-0.1199928	1.473343	0.2248723
3	-3.449391e-3	0.3609992	1.121988	-0.3094506	1.473360	0.2248829
4	9.381872e-4	0.3600937	1.122277	0.1868954	1.489204	0.2327578
5	8.944660e-4	0.3592776	1.122539	2.722244e-10	4.498694	0.5419195
6	8.683892e-4	0.3587206	1.122718	3.437098e-20	1.959055	3.747129
$k = 2$						
1	1.030832e-3	2.196770	0.7149692	4.802783e-3	0.3880369	0.2112838
2	-5.817601e-3	2.259210	0.7201542	6.225231e-4	1.664431	0.3283672
3	4.818115e-3	2.269287	0.7209898	6.642306e-2	-4.561958	0.3390357
4	1.956628e-5	1.665406	1.619418	7.858702e-10	5.262455	0.4312077
5	-5.438509e-5	1.664943	1.619572	3.935674e-7	2.940227	0.9450288
6	3.482543e-5	1.664755	1.619634	6.684828e-21	2.846936	4.072948

**Table A.5.** GP coefficients, corresponding to the Equation (10) for  $D^k(j = N + 1, T)$ , are provided for rotational levels within the  $\Pi$ -state, with  $k$  equal to 1 and 2.

$i$	$a_i^k$	$j^{\alpha_i^k}$	$\beta_i^k$	$b_i^k$	$\gamma_i^k$	$\delta_i^k$
$k = 1$						
1	2.881511e-5	0.6858308	1.280080	-7.963110e-4	1.455747	0.8831807
2	-9.313931e-5	0.6702042	1.280779	7.962892e-4	1.455742	0.8831870
3	1.573687e-4	0.6529715	1.281580	5.486403e-12	3.246100	0.9696506
4	-9.304530e-5	0.6458879	1.281917	9.461886e-25	1.289088	4.593579
$k = 2$						
1	7.778896e-5	1.148716	1.056787	1.469117e-7	2.926629	0.6638563
2	-2.744207e-4	1.062771	1.070655	-1.371769e-2	1.264619	0.6899927
3	3.058522e-5	1.033921	1.075424	1.636800e-2	1.282435	0.6957809
4	1.687107e-4	1.015060	1.078548	4.727379e-3	-2.247660	0.7048250
5	-7.833470e-18	0.1888026	3.768634	-2.842829e-3	1.348965	0.7114709

**Table A.6.** GP coefficients associated to Equation (10) for  $D^k(j = N \rightarrow j' = N' = N+2, T)$  are given for rotational levels within the  $\Pi$ -state, where  $k$  equals 0, 1 and 2.

$i$	$a_i^k$	$j^{\alpha_i^k}$	$\beta_i^k$	$b_i^k$	$\gamma_i^k$	$\delta_i^k$
$k = 0$						
1	8.131733e-2	1.368889	0.4501252	2.579855e-2	2.216276	-0.2126671
2	1.854918e-3	1.481682	0.6827418	0.1051687	1.231380	0.4790863
3	7.145952e-4	1.226836	1.089026	3.530731e-2	0.2205783	0.6630505
4	6.316946e-4	1.250177	1.112160	1.052831e-7	1.207201	1.834124
$k = 1$						
1	-9.236490e-11	0.9900076	2.855520	3.553307e-3	0.9487627	0.8797230
2	6.004538e-5	0.9881903	1.302873	1.111160e-2	1.078368	0.6830387
3	4.043410e-5	1.088956	1.428987	1.273399e-2	0.8321978	0.6906823
4	4.497109e-6	0.9870536	1.759647	5.572296e-3	0.9256184	0.8196994
5	-8.575254e-6	0	1.555283	1.402920e-2	1.057578	0.6979735
6	1.971299e-2	1.010017	0.9322726	0.2245883	0	0.6259280
$k = 2$						
1	4.613728e-2	1.007588	0.8005586	0.2866146	1.144674	0.1364757
2	-2.640124e-2	0.8563931	0.8711782	4.477300e-2	0.4118615	0.4724249
3	8.9231410e-6	1.019305	1.596336	8.635446e-3	1.130790	0.6933346
4	-4.865965e-11	1.043426	2.764539	1.102920e-3	0.7979468	0.8035571